JOURNAL OF SOLID STATE CHEMISTRY 1, 195–204 (1970)

Fluorine-19 NMR Relaxation Studies in the Tungsten Fluoroxide Bronzes†

J. C. GULICK‡ AND M. J. SIENKO

Department of Chemistry, Cornell University, Ithaca, New York 14850

Received August 1, 1969

Compounds of the type $K_xWO_{3-y}F_y$ have been prepared by solid-state reaction of KF, WO_3, and W at 900°. X-ray powder diffraction patterns correspond closely to those of hexagonal, tetragonal, and cubic potassium tungsten bronzes. The magnetic susceptibility of $K_{0.1}WO_{2.9}F_{0.1}$, as measured with a vibrating sample magnetometer, shows a very small, temperature-independent paramagnetism. Fluorine-19 NMR studies have been carried out on a series of mixtures with x and y lying between 0.014 and 0.16. Knight shifts, measured at 298°K and 77°K, were less than $0.001 \pm 0.001\%$. Spin-lattice relaxation times, T_1, measured as a function of temperature over the range 1.2–298°K by a continuous-wave, fast-passage technique and a 90°–90° pulse method, were observed to be proportional to inverse temperature for both $K_{0.014}WO_{2.91}F_{0.09}$ and $K_{0.1}WO_{2.84}F_{0.16}$ but proportional to $T^{-1/2}$ for $K_{0.056}WO_{2.89}F_{0.11}$. At 2.1°K, T_1 ranges from 2 sec to 300 sec, increasing with decreasing fluorine-plus-potassium content. Spin-spin relaxation times, T_2, determined from free-induction decay and from the NMR line-width, are of the order of 100 μsec, decreasing with increasing fluorine-plus-potassium content and with decreasing temperature. Results suggest a conduction-electron relaxation mechanism for the ^{19}F resonance and are consistent with a tungsten $5d(t_{2g})$–oxygen $p\pi$ overlap model for the conduction band in the tungsten bronzes.

Introduction

The tungsten bronzes, M_xWO_3, are nonstoichiometric compounds in which M (an alkali metal, alkaline earth metal, lanthanoid, Pb, Tl, H, or NH_4) is an interstitial dopant in a tungsten-oxygen matrix derived from the insulator WO_3 (*1*). When the concentration of M is small, the bronzes are semiconducting (*2*), but when x exceeds about 0.25 the behavior is generally metallic. Arguments in favor of a change from localized to delocalized electrons at $x = 0.25$ have been given on the basis of a simple Mott theory (*3*). In the metallic region, magnetic susceptibility (*4*), single-crystal conductivity (*5*), Hall voltage (*6*), and Seebeck effect (*7*) agree quite well with a slightly modified free-electron theory. A quantitative fit of conductivity and Seebeck coefficient as functions of temperature and concentration has been obtained for Na_xWO_3 using the perturbation theory of Howarth and Sondheimer for polar scattering by optical-mode lattice vibrations in the limit of high degeneracy (*8*).

Still, the nature of the conduction band has not been settled. Mackintosh (*9*) proposed for Na_xWO_3 the use of sodium wave functions. That these are not 3*s* functions can be deduced from an observed absence of a ^{23}Na Knight shift (*10*). Neither does it seem likely, as suggested by Mackintosh, that they are 3*p* functions, lowered by the crystal field enough below the 3*s* levels to exclude practically all 3*s* character. Finally, the observation by Ferretti, Rogers, and Goodenough (*11*) that pure stoichiometric ReO_3 shows metallic conductivity, even without the presence of alkali doping, conclusively excludes the need of using alkali-atom wave functions.

Keller, on the other hand, has suggested that the conduction band is composed of tungsten 6*s* functions (*12*). That this is not the case is shown by the NMR studies of Narath and Wallace (*13*) who found no Knight shift for the ^{183}W resonance, as would have been the case if there were finite conduction-electron density at the tungsten nucleus. Rather, by correlating the resonance shift with the

† This research was sponsored by the U.S. Air Force Office of Scientific Research, Office of Aerospace Research, U.S. Air Force, under AFOSR Grant Number 796-67 and was supported in part by the National Science Foundation and the Advanced Research Projects Agency through the Materials Science Center at Cornell University. This report is based in part on the Ph.D. Thesis of J. Gulick.

‡ Present address: Department of Chemistry, Florida State University, Tallahassee, Florida 32306.

electronic specific heat measured by Vest, Griffel, and Smith, (*14*) they concluded that non-*s* tungsten states contribute significantly to the conduction-band states. Following the work of Morin (*15*) on 3*d* oxides, Sienko (*16*) has suggested that the WO_3 conduction band arises from overlap of the three $5d(t_{2g})$ orbitals of a tungsten atom. Goodenough (*17*), on the otherhand, believes that tungsten-tungsten separation is too large to give direct overlap of the 5*d* orbitals and that a π band involving mixing of W 5*d* and oxygen $p\pi$ orbitals is more likely. Gerstein, Thomas, and Silver (*18*) have calculated overlaps for the cubic sodium tungsten bronzes using Slater orbitals with exponents adjusted to match SCF functions and find from overlap considerations alone that a conduction band formed from d-$p\pi$ mixing of tungsten and oxygen orbitals is reasonable. The degree of W–O mixing is, however, attenuated by the large energy difference between the two sets of orbitals (*19*). For this reason, the direct overlap band arising from equal-energy $5d(t_{2g})$ orbitals on adjacent tungsten atoms cannot automatically be rejected as an appropriate description for the conduction electrons in tungsten bronzes.

In an attempt to decide between d-d and d-O$p\pi$-d overlap models, this investigation was undertaken to exploit NMR as a technique for defining electron density variations at magnetic nuclei. Since ^{17}O was not economically feasible as a suitable probe, ^{19}F substituted for oxygen was chosen on the assumption that, although F is more electronegative than O, little perturbation of the band structure would occur if the amount of F substitution were kept small. No ^{19}F Knight shift from the conduction electrons was expected because of the p-orbital node at the nucleus, although a small negative shift could occur as a result of core polarization. The main thrust of the investigation was to examine the behavior of the spin-lattice relaxation time T_1. For conduction-electron relaxation, T_1 is inversely proportional to temperature; relaxation due to paramagnetic impurities is independent of temperature, and relaxation through lattice vibrations is much slower than would be expected for conduction electrons. Finally, since T_1 is a function of the density of states in a conduction-electron mechanism, it is expected to decrease with increasing concentration of electrons in the conduction band. The following report describes the preparation, characterization, and study of magnetic and magnetic-resonance properties of fluoride-doped tungsten bronzes.

Experimental

Preparation

Mixtures of W, WO_3, and alkali fluoride were ground together in an agate mortar in proportions to yield compounds of the formula $M_xWO_{3-x}F_x$. Reagent grade chemicals were used throughout except for the WO_3 which was Fisher "purified". Mixtures were sealed in evacuated platinum capsules and heated and cooled under varying conditions of temperature, reaction time, and cooling rate. Some of the mixtures were reground and reheated, but even then products were generally mixtures having X-ray powder patterns corresponding to the tungsten bronzes or the reduced tungsten oxides. In a typical reaction, heating was continued for 30 hr at 900°, followed by cooling at 20° per hr.

Analysis

The series of compounds from the capsule reactions was analyzed by the Analytical Facility of the Cornell University Materials Science Center. Results of the analyses are shown in Table I. Calculated compositions are based on proportions of starting material. All samples were water-washed

TABLE I

CHEMICAL ANALYSIS OF POTASSIUM FLUOROXIDE BRONZES

Designation	Nominal composition	% Found			Actual composition
		W	F	K	
(*C*)	$K_{0.075}WO_{2.925}F_{0.075}$	75.9 ± 0.4	0.68	0.23	$K_{0.014}WO_{2.91}F_{0.086}$
(*D*)	$K_{0.1}WO_{2.9}F_{0.1}$	73.9	0.87	0.88	$K_{0.056}WO_{2.89}F_{0.11}$
(*E*)	$K_{0.11}WO_{2.89}F_{0.11}$	76.0	1.03	—	$K_{0.11}WO_{2.87}F_{0.13}$
(*F*)	$K_{0.15}WO_{2.85}F_{0.15}$	90.5	0.96	4.08	$K_{0.3}WO_{2.84}F_{0.16}$
(*B*)	$K_{0.15}WO_{2.85}F_{0.15}$	77.7 ± 1.6	1.27 ± 0.06	1.64	$K_{0.1}WO_{2.84}F_{0.16}$

prior to analysis: samples (C), (D), and (F) were also leached in aqueous HF for 5 days.

Fluoride was determined by direct potentiometric measurement of fluoride activity with an Orion (*20*) ion-selective electrode using the method of Raby and Sunderland (*21*). Tungsten and potassium were determined by thiocyanate colorimetry and flame photometry, respectively. In all cases, authentic standards were prepared by treating mixtures of NaF and Na_2WO_4 in the same manner as the unknowns.

Samples for fluoride analyses were fluxed with a mixture of NaOH and $NaNO_3$ at 500° and then dissolved in distilled water. Since the fluoride electrode responds to fluoride activity, not concentration, the ionic strength and pH were carefully controlled during these analyses. There are no known interferences with this method of fluoride determination.

The erratic nature of the analytical results is believed to be due in part to incomplete reaction and in part to local variations in sample composition. Although the fluoride and potassium analyses appear self-consistent within moderate limits of error, the tungsten analysis appears to be less reliable. Repeated tungsten analyses on the same solution were reproducible to a few percent, but results from different samples of the same material varied widely. Sample inhomogeneity could well be the decisive factor.

The sum of potassium and fluoride content for the sample of nominal composition $K_{0.1}W_{2.9}F_{0.1}$ was confirmed by measurement of total reducing power. Two samples of the bronze were dissolved in K_2CO_3 solution containing $Ag(CNS)_4^{3-}$, and the precipitated silver was collected, dissolved in nitric acid, and determined by the Volhard method. The reducing power—i.e., the number of moles of electrons that can react with oxidizing agent per mole of compound—was found to be 0.147 and 0.148 in the replicate runs, compared to 0.166 for the calculated value.

X-ray Analysis

Powder diffraction patterns were obtained with a General Electric XRD-5 diffractometer using Ni-filtered copper Kα radiation. Chart recordings were made at scan rates of 2° per minute and 0.4° per minute. The diffractometer 2θ-scale was calibrated with W and WO_3 powders. The rate meter was arbitrarily biased to place all background near zero. Intensities were normalized to the height of the strongest line. Patterns were assigned with moderate success on the basis of hexagonal plus either tetragonal or cubic unit cells. A few low-intensity lines at low angles, possibly due to tungstates, polytungstates, or fluorotungstates, could not be assigned. Typical line assignments, 2θ-values, intensity, and $\sin^2\theta$-values are shown in Table II, corresponding in this case to Sample *C*, $K_{0.075}WO_{2.925}F_{0.075}$. Table III gives the lattice parameters as determined for the samples used in the nuclear resonance studies. The X-ray pattern indicates that the compound of nominal formula $K_{0.30}WO_{2.70}F_{0.30}$ is entirely one phase, though the material itself appears to be a mixture of a red phase and a blue phase which if analogous to the pure potassium tungsten oxide bronzes are a tetragonal and hexagonal phase, respectively. Apparently, the tetragonal phase was not in high enough concentration to appear in the X-ray data.

Magnetic Susceptibility

Magnetic susceptibilities were measured with a Princeton Applied Research Parallel Field Vibrating Sample Magnetometer, Model 150. The instrument, a prototype still under development, was equipped with a superconducting solenoid in which the sample in a lucite or nylon holder was vibrated by coupling to the diaphragm of a radio speaker. The voltage induced in a set of stationary pick-up coils was detected and amplified by a phase-sensitive lock-in amplifier. Temperature control was provided by helium gas derived from bleeding liquid helium from the magnet chamber through a capillary tube into the sample chamber. A small heater wound around the capillary allowed the entering gas to be warmed from liquid helium temperature to about 300°K. The temperature of the sample chamber was monitored by four sensors: two copper-constantan thermocouples, a gallium-arsenide diode, and a carbon resistor.

Magnetic-moment measurements as a function of temperature were made for two samples of nominal composition $K_{0.09}WO_{2.91}F_{0.09}$ and $Na_{0.1}WO_{2.9}F_{0.1}$. The instrument was calibrated with a small pellet of nickel. Measurements were made between 4.2° and 300°K at a field strength of 33 kG for the sodium sample and 16.5 kG for the potassium sample. Although there is a large scatter in the results, the magnetic behavior of the fluoride-doped bronzes is similar to that of the tungsten bronzes. There was no reproducible change of magnetic moment with temperature and the magnitude is of the same order—e.g., $\chi_M = 10 \times 10^{-6}$, for $Na_{0.1}WO_{2.9}F_{0.1}$. Despite difficulties encountered in use of an unproven instrument, the sensitivity of the device was notable. It is unlikely that susceptibility measure-

TABLE II

X-RAY POWDER DIFFRACTION DATA, $K_{0.075}WO_{2.925}F_{0.075}(C)$

2θ	Intensity	$\sin^2\theta$ (Obsd.)	$\sin^2\theta$ (Calc. hex)	*hkl*	$\sin^2\theta$ (Calc. tetr)	*hkl*
13.8	44	0.0144	0.0145	100		
23.0	100	0.0399	0.0400	002	0.0405	001
23.8	100	0.0425			0.0428	200
			0.0435	110		
24.9	13	0.0465				
26.8	14	0.0537	0.0535	111	0.0535	210
27.8	70	0.0577	0.0580	200		
28.6	24	0.0610			0.0619	111
33.4	40	0.0826	0.0835	112	0.0833	201
34.1	26	0.0860			0.0856	220
36.8	25	0.0996	0.1000	202		
39.2	12	0.1125	0.1120	211		
41.5	16	0.1255			0.1261	221
42.3	17	0.1302	0.1305	300		
45.2	13	0.1477			0.1475	311
47.0	20	0.1590	0.1600	004		
48.8	25	0.1707	0.1705	302	0.1714	400
49.3	31	0.1740	0.1740	220		
50.3	22	0.1806			0.1796	321
51.4	14	0.1881	0.1885	310		
53.3	18	0.2012				
54.8	22	0.2118	0.2115	114	0.2117	401
56.7	14	0.2255	0.2260	204		
57.4	20	0.2306	0.2320	400		
59.4	12	0.2455			0.2476	222

TABLE III

LATTICE PARAMETERS (Å)

Sample (nominal composition)	Hexagonal phase	Cubic or tetragonal phase
$K_{0.075}WO_{2.925}F_{0.075}$	$a_0 = 7.43$, $c_0 = 7.69$	$a_0 = 7.45$, $c_0 = 3.83$
$K_{0.1}WO_{2.9}F_{0.1}$	$a_0 = 7.38$, $c_0 = 7.50$	$a_0 = 3.83$, $c_0 = 3.73$
$K_{0.11}WO_{2.89}F_{0.11}$	$a_0 = 7.43$, $c_0 = 7.50$	$a_0 = 7.64$, $c_0 = 7.45$
$K_{0.15}WO_{2.85}F_{0.15}$	$a_0 = 7.38$, $c_0 = 7.59$	$a_0 = 3.80$
$K_{0.3}WO_{2.7}F_{0.3}$	$a_0 = 7.43$, $c_0 = 7.69$	none

ments could have been made on these small samples of materials with small moments by any other method.

Nuclear Magnetic Resonance

Continuous-wave NMR measurements were obtained with a Varian spectrometer and probe and a Princeton Applied Research lock-in amplifier for phase-sensitive detection. The radiofrequency was 16 MHz for Knight shift measurements and 8 MHz for fast-passage measurements of the spin-lattice relaxation time T_1. A saturated KF solution served as the fluorine reference signal in the Knight shift measurements. Knight shift spectra were recorded

TABLE IV

RELAXATION TIME DATA FROM PULSE EXPERIMENTS

Sample	Temperature (°K)	T_1 (Sec)	T_1T (Sec°K)	T_2 (μsec)
(*C*)	77	3.3 ± 1	254	250 ± 70
	4.2	100 ± 20	420	100 ± 15
	2.1	280 ± 50		
(*D*)	77	3.4 ± 0.4	261	100 ± 40
	4.2	17 ± 2	71.4	100 ± 15
	2.1	24 ± 3	52.5	100 ± 15
	1.2	28 ± 2	33.6	90 ± 5
(*B*)	77	3 ± 1	154	200 ± 30
	4.2	6.3 ± 1	26.4	50 ± 10
	2.1	11 ± 2	22.0	50 ± 5
	1.2	19 ± 6	22.8	50 ± 5
(*F*)	4.2	3.0 ± 0.4	12.6	~ 60
	2.0	1.5 ± 0.5	3.0	$\leqslant 15$

on an x-y recorder with the x-axis driven by the retransmitting potentiometer of the Fieldial. Procedure was to sweep first through the KF reference line, replace the standard in the probe by the fluoroxide bronze, sweep through the bronze signal, and then repeat with the KF standard. Shift of the bronze line was determined with respect to the average of the two KF spectra.

The spin-lattice relaxation time was measured at 77°K by the fast-passage technique (*22*). In this method the nuclear magnetization, M, is reversed by sweeping the DC field, H_0, through the resonance value, $H_0^* = -\omega/\gamma$, in the presence of a relatively large rf field, H_1, of frequency ω. The signal is observed at two consecutive fast-passages separated by time t. The first signal, at time $t = 0$, corresponds to a transverse magnetization equal to M_0. At the end of the passage $M_z = M_0$, and t seconds later $M_z = M_0[1 - 2\exp(-t/T_1)]$. The signal of the second fast passage is proportional to $-M_z$, the negative sign being due to the fact that the first and second signals are observed starting from opposite sides of the resonance. Using rf fields of about 1 G and sweep rates of 250 G/min, T_1 was determined at 77°K to be about 2.3 sec, for $K_{0.056}WO_{2.89}F_{0.11}$ (Sample *D*) and about 3.5 sec, for $K_{0.014}WO_{2.91}F_{0.086}$ (Sample *C*). Figure 1 shows the plots of natural log magnetization vs. time from which the relaxation times were determined.

At liquid-helium temperatures spin-lattice relaxation times were determined by a pulse method in which the return is measured of the nuclear spin

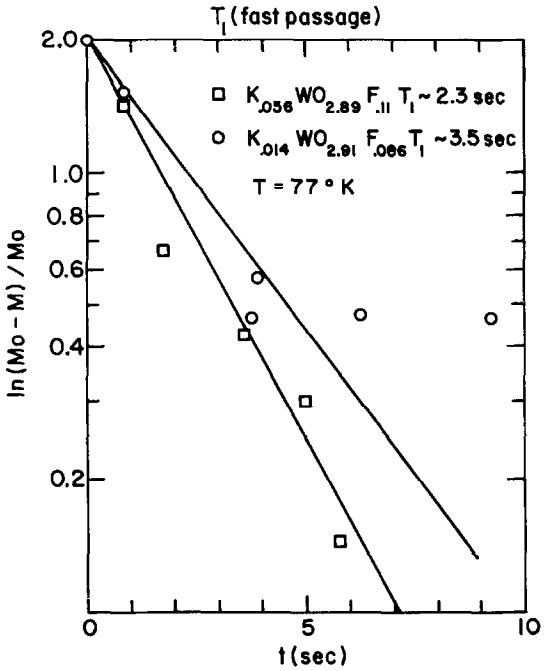

FIG. 1. Plot of natural log magnetization vs. time for determination of spin-lattice relaxation time T_1 by fast-passage technique.

system to thermal equilibrium after a 90° pulse. A 90°, or "killing", pulse is applied by chosing t_w, the duration of an rf pulse, and H_1, the strength of the rf field, so that $\gamma H_1 t_w = \pi/2$, destroying magnetization in the z direction by nutating the spins into the

x-y plane. At time t after the killing pulse, when some of the magnetization has reformed in the z direction, a second 90° pulse is applied to tip whatever portion of the magnetization has recovered back into the x-y plane. Immediately after the second pulse the signal is given by $M_t = M_0[1 - \exp(-t/T_1)]$, and a plot of $\ln[(M_0 - M_t)/M_0]$ vs. t gives a straight line of slope $-T_1^{-1}$. Figure 2 shows representative data for $K_{0.1}WO_{2.84}F_{0.16}$ (Sample B).

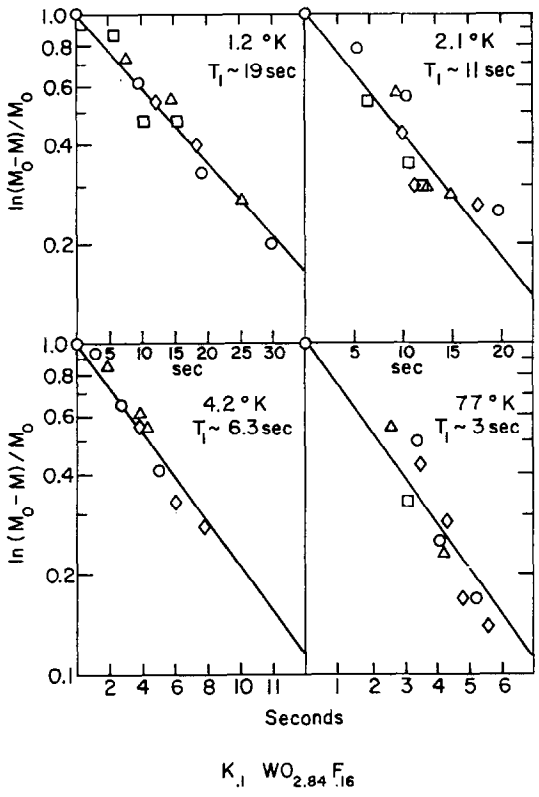

FIG. 2. Plot of natural log magnetization vs. time for determination of spin-lattice relaxation time T_1 by 90°–90° pulse technique. Sample composition corresponds to $K_{0.1}WO_{2.84}F_{0.16}$ (Sample B).

A block diagram of the pulse apparatus is shown in Fig. 3. Part of the output of a continuously-running master oscillator set at about 16 MHz is fed to a phase shifter and then to a gate circuit which opens on the arrival of a pulse from the timing circuits and stays open for the length of the pulse. While the gate is open the rf signal reaches a transmitter which amplifies the pulse and puts about 2 kV peak voltage across a transmitter coil. A receiver coil, approximately perpendicular to the transmitter coil senses the nuclear signal and sends it to a receiver by which it is first amplified and then phase-sensitive detected. The other part of the output of the master oscillator goes to the receiver and provides for the phase-coherent detection. After detection, the signal is observed on an oscilloscope where it is photographed by a camera mounted on the scope. The pulse apparatus is similar in design to that built by Clark (*23*) and modified by Wayne (*24*).

Spin-spin relaxation times, T_2, were determined from the free-induction decay. Signals were observed about 10 kHz off resonance. The magnetic moment precesses with angular frequency γH_0 giving a nuclear-induction signal that beats with the rf reference signal. Since phase coherence persists for a time of the order of T_2, there is an exponential decay of the beat signal with characteristic time T_2. A plot of the natural log of beat intensity as a

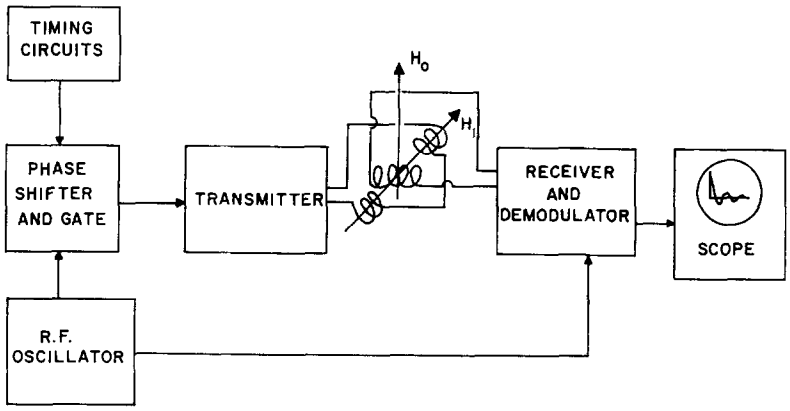

FIG. 3. Components of apparatus for determining spin-lattice relaxation time by 90°–90° pulse technique. The sample is in the coil in the lab field H_0. The H_1 represents the rf field applied by the crossed coils.

function of time gives a straight line with slope $-T_2^{-1}$. Figure 4 shows representative data for $K_{0.1}WO_{2.84}F_{0.16}$ (Sample *B*). Values for T_2 are order of magnitude guesses at 77°K, but improve in accuracy with improved signal at lower temperature.

Table III collects the data obtained for T_1, T_2, and T_1T as determined from pulse experiments for the four samples investigated by this technique. Figure 5 gives a logarithmic plot of the T_1 vs. T data. For Samples *B* and *C*, T_1 is close to inversely proportional to temperature at 4.2°K and below, whereas for Sample *D*, T_1 is approximately proportional to $T^{-1/2}$. There are not enough data for Sample *F* to establish a trend.

Discussion

There are several relaxation mechanisms by which nuclear spins can reach thermal equilibrium with the lattice: interactions with conduction electrons in metals, interactions with paramagnetic centers, and lattice vibrations. In a metal, when an electron passes close to a nucleus, the nucleus experiences a relatively large time-varying field which may induce transitions between the magnetic-energy sublevels of the nucleus, thus providing a relaxation path. The energy, $h\nu$, emitted or absorbed by the nucleus is taken up or surrendered by the electron by adjustment of its kinetic energy. Such a transition is possible only when there are vacant levels available to the electron—i.e., at the top of the energy distribution within a range of the order of kT of the Fermi level, E_0. Since $h\nu \ll kT$, only kT/E_0 of the electrons can interact with the nuclei, or about 1 % at room temperature. The probability of such a transition, W, is also related to the magnetic-interaction energy, E_1, between the magnetic moment of the electron, μ_e, and the magnetic moment of the nucleus, μ_n, at their distance of closest approach, r_{12}. In its most general form (*25*), it can be expressed as follows:

$$W = 1/2T_1 = (3\pi^2/8)^{1/3} E_1^{\,2} kT/E_0^{\,2} \hbar;$$
$$E_1 \cong \mu_e \mu_n / r_{12}^3.$$

Thus, there is an r^{-6} dependence on separation of the dipolar spin-lattice relaxation rate for non-*s* electrons. Therefore, sodium 3*p* conduction electrons at the Fermi surface can provide a significant relaxation mechanism for ^{23}Na nuclei. Similarly, tungsten 5*d* conduction electrons can provide a significant relaxation mechanism for ^{183}W nuclei without appreciably affecting the sodium nuclei (*26*).

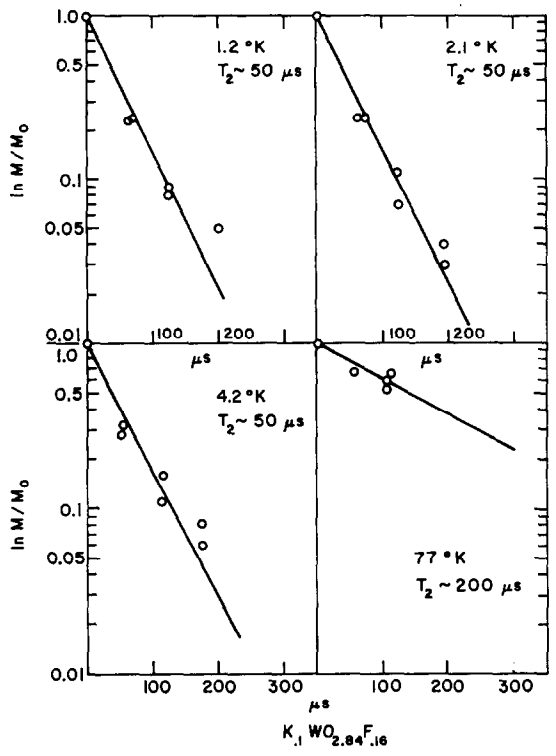

FIG. 4. Plot of natural log magnetization vs. time for determination of spin-spin relaxation time T_2 by free-induction decay. Sample composition corresponds to $K_{0.1}WO_{2.84}F_{0.16}$ (Sample *B*).

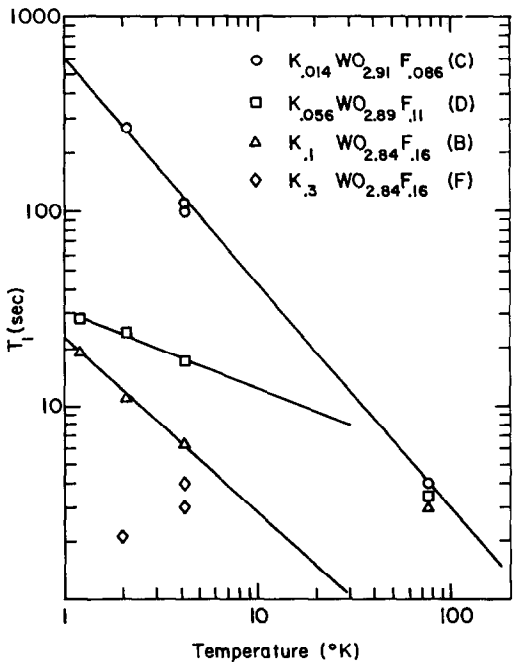

FIG. 5. Logarithmic plot of spin-lattice relaxation time T_1 vs. temperature for four fluoroxide bronzes.

It is also reasonable to expect that tungsten 5*d* electrons would have little effect on the ^{19}F relaxation, whereas fluorine 2*p* conduction electrons would have a large contribution to the ^{19}F relaxation.

The contributions to relaxation rates in solids have complicated dependences. In well-characterized systems it is possible to calculate the contribution via contact interactions, core polarization, orbital interactions (i.e., interaction with the orbital momentum of unpaired non-*s* electrons), and spin-dipolar interactions. The separate contributions have been calculated by Yafet and Jaccarino (*27*) and by Obata (*28*) from the density of states at the Fermi level and fractional admixtures of *d*, *p*, and *s* states at the Fermi surface. However, there are too many variables in the bronze system, and the data are not enough to separate these. Nevertheless, the conduction-electron effects are inversely proportional to temperature (i.e., $T_1 \propto T^{-1}$), so it is possible to make some conclusions from the data available.

Other relaxation mechanisms include exchange of energy with lattice vibrations and energy exchange with paramagnetic impurities. Relaxation through lattice vibrations would predict relaxation times which are long (about 10^4 sec at room temperature) and proportional to T^{-2}. Relaxation through paramagnetic impurities would predict relaxation times that are inversely proportional to concentration and independent of temperature (*29*).

The temperature dependence of T_1 in Samples *B* and *C* is approximately inversely proportional to temperature. This behavior is expected if the predominant relaxation mechanism is transfer of energy to conduction electrons. If this were the *only* mechanism and if core polarization—i.e., contact interaction resulting from polarization of core *s* electrons by non-*s* conduction electrons—were the only important conduction-electron perturbation acting on the spin system then one would expect the Korringa-like relation:

$$T_1 TK^2 = h\gamma_e^2/4\pi kq\gamma_n^2,$$

obtained by Yafet and Jaccarino (*27*) to give an estimate of the relationship between the Knight shift *K* and T_1. Here *q* is a reduction factor which is given by the reciprocal of the orbital degeneracy of the conduction band. Calculation of the Knight shifts from T_1 values at 77°K gives results of the same order of magnitude as the observed shifts—i.e., $\pm 0.001\%$, or within the experimental uncertainty. (Orbital contributions to the Knight shift would be positive and tend to cancel the effects of core polarization. There are not enough data to separate the effects, however.) Deviations from linearity in T_1 vs. *T* plots indicate the presence of more than one relaxation mechanism or more than one kind of fluorine.

Abragam (*30*) has derived the theoretical dependence of T_1 on *T* for a semiconductor using Boltzmann statistics, where the small density of electrons in the conduction band makes the electron gas nondegenerate; the result was $T_1 \propto T^{-1/2}$.

In Samples *B* and *C* the temperature dependence of T_1, is clearly that of a metallic, conduction-electron relaxation mechanism, and not that of a semiconductor. Generally the tungsten bronzes with $x < 0.25$ are semiconductors; in the fluoride bronzes, however, it is necessary to consider not fluorine or alkali metal concentration alone, but the combination of the two since one electron is contributed by each fluorine and each alkali atom. In Sample *B* total reducing power, which is analogous to *x* for nonfluoride bronzes, equals 0.26; in *C*, it is 0.1; in *D*, it is 0.17; and in *F* it is 0.36. The data suggest that Sample *C* and possibly also Sample *B* undergo a semiconductor metal transition on cooling from room temperature to 4.2°K. Without pure compounds or single-crystal resistivity data, this suggestion is speculative.

In Sample *D* the temperature dependence of T_1 does appear to be that of a semiconductor. It is not clear why there should be such a difference in behavior among the three samples. The chemical composition of *D* is intermediate between those of *B* and *C*, but the crystal structures are different in the three mixtures. All contain the same hexagonal phase, but the second phase in each sample is different. Sample *B* contains a small amount of cubic material and *C* and *D* contain *different* tetragonal materials. It is not possible to tell whether one phase or another is fluoride-rich, but one could speculate that the dominant fluoride phases in Samples *B* and *C* underwent transitions from semiconducting to metallic states, whereas the fluoride-rich phase of Sample *D* did not undergo such a transition. Thus, the data are not necessarily inconsistent.

In Sample *F*, T_1 is temperature independent within experimental error. This is the only one of the four samples with a reducing power significantly greater than 0.25. It is also the only sample with a single phase X-ray diffraction pattern, a hexagonal phase similar to that of the potassium tungsten bronzes. Remeika *et al.* (*31*) have found that hexagonal potassium bronzes which have been etched in HF become superconducting in the temperature range

5.70–3.31°K. Since Sample *F*, like *C* and *D* but unlike *B*, was leached for five days in HF, it may be that in *F* a superconducting phase exists at temperatures less than 4.2°K. Above this temperature lines would be broadened by the presence of random distribution of potassium ions around the fluorines. As the temperature is lowered, T_1 would remain short because of the high concentration of electrons at the Fermi level. The T_1 for a metal increases as the temperature drops, but it has been observed in aluminum that if there is a transition to a superconducting state T_1 decreases sharply and then slowly begins to increase again (*32*). The signals from a superconductor would probably be very weak unless the powder were very finely ground because of skin effects which prevent penetration of the rf radiation into the sample.

As a general result for the four samples, the dependence of T_1T on reducing power is consistent with a conduction-electron relaxation mechanism. The increase in relaxation rate with increasing potassium plus fluorine content is to be expected from an increase in the density of states at the Fermi level as the band is filled. Although the lack of data on pure compounds allows only qualitative comparisons, the relaxation rates appear to be strongly dependent on reducing power and to be relatively short.

The T_1T for ^{19}F is comparable to that found for ^{183}W in Na_xWO_3 (*26*); i.e., 6.8 sec°K at $x = 0.89$, and 15.3 sec°K at $x = 0.56$. The T_1T data for ^{19}F are not available in this range of x values, but for reducing power $x = 0.26$, T_1T is approximately equal to 22 sec°K; for $x = 0.17$, about 50 sec°K; and for $x = 0.46$, in the range 3.0–17 sec°K. We conclude then that at a given reducing value T_1T values are about the same order of magnitude for the W and F nuclei.

However, one cannot directly compare T_1T values for different nuclei without taking account of the different magnetic moments of the nuclei. From the equation above for the transition probability W we get:

$$1/T_1T \propto \mu_e^2\mu_n^2/r^6,$$

or, more correctly (*27*, *28*), using the squared expectation value of r^{-3} in place of r^{-6},

$$1/T_1T \propto \mu_e^2\mu_n^2\langle r^{-3}\rangle^2.$$

The comparison between relaxation times for ^{183}W and ^{19}F can be written:

$$(T_1T)_W/(T_1T)_F = \mu_F^2\langle r^{-3}\rangle_F^2/\mu_W^2\langle r^{-3}\rangle_W^2,$$

where, using 2.63 and 0.115 for the nuclear moments of fluorine and tungsten, respectively, $\mu_F^2/\mu_W^2 = 525$. For $\langle r^{-3}\rangle_W$ we can take the value 7.5 a.u. from the estimate by Low (*33*) for W^{5+} on the basis of electron paramagnetic resonance data. (A smaller value might possibly be more appropriate for the fluoroxide bronzes, since the electrons are apparently not localized on the tungsten atoms.) For fluorine, the value of $\langle r^{-3}\rangle_F$ depends on the model chosen. If the fluorine does *not* participate in conduction-band formation—i.e., if the conduction band is formed by $Wt_{2g} - t_{2g}$ overlap only—then an average ^{19}F-to-electron distance can be approximated by the distance between ^{19}F and a line joining two diagonally opposite tungsten atoms. In an idealized perovskite unit cell with $a_0 = 3.80$ Å, this distance would be 1.34 Å. If we take $\langle r^{-3}\rangle_F = (1.34\text{ Å})^{-3} = 0.062$ a.u. then we would calculate

$$(T_1T)_W/(T_1T)_F \cong 525\,(0.062/7.5)^2 \cong 1/28.$$

The fact that $(T_1T)_W/(T_1T)_F$ is actually closer to unity suggests that the fluorine does indeed participate in the conduction band.

The above calculation is but approximate since it is quite sensitive to the choice of value for $\langle r^{-3}\rangle_W$. The value chosen was the only published value available; if a value were estimated by comparison with other Group VI transition metals (*34*), $\langle r^{-3}\rangle$ might be between 3 and 4 a.u., in which case $(T_1T)_F$ would be calculated to be about 5–12 times $(T_1T)_W$. Similarly if $\langle r^{-3}\rangle_F$ were taken to be 8.9 a.u., the value for $2p$ orbital of fluorine (*35*), then $(T_1T)_W$ would be 750 $(T_1T)_F$. The observed values of T_1 for ^{19}F are nowhere near this short, but since the conduction band is presumed to be a $p\pi^*$ band the expectation value of r^{-3} would be changed in the direction of $r > r_{2p}$, hence bringing $(T_1T)_F$ closer to the value of $(T_1T)_W$.

At present there are too many parameters and unknowns in the fluoroxide bronzes to state unequivocally that the $Wt_{2g} - t_{2g}$ band model must be discarded. However, the data suggest that some p orbital contribution to the conduction band is necessary to account for the relaxation times observed.

Acknowledgment

We should like to express our appreciation to Robert Wright and the Prince Applied Research Corporation for the opportunity to use the PAR Model 150 Vibrating Sample Magnetometer while it was under development. We also thank James Murday for obtaining the NMR data and for much useful advice in interpreting the results. Finally, we acknowledge our deep appreciation to Prof. Robert Cotts for his valuable counsel and suggestions.

References

1. For reviews on the tungsten bronzes, see M. J. SIENKO, *Adv. in Chem. Ser.* **39**, 224 (1963); "The Alkali Metals", pp. 429–451, Special Publication No. 22, Chemical Society (London, 1967); P. G. DICKENS AND M. S. WHITTINGHAM, *Quart. Rev. (London)* **22**, 30 (1968).
2. W. MCNEILL AND L. E. CONROY, *J. Chem. Phys.* **36**, 87 (1962); H. R. SHANKS, P. H. SIDLES, AND G. C. DANIELSON, *Advan. Chem. Ser.* **39**, 237 (1963).
3. M. J. SIENKO AND T. B. N. TRUONG, *J. Am. Chem. Soc.* **83**, 3939 (1961).
4. P. M. STUBBIN AND D. P. MELLOR, *Proc. Roy. Soc. N. S. Wales*, **36**, 772 (1948); L. E. CONROY AND M. J. SIENKO, *J. Am. Chem. Soc.* **79**, 4048 (1957); J. D. GREINER, H. R. SHANKS, AND D. C. WALLACE, *J. Chem. Phys.* **36**, 772 (1962).
5. E. J. HUIBREGTSE, D. B. BARKER, AND G. C. DANIELSON, *Phys. Rev.* **84**, 142 (1951); L. D. ELLERBECK, H. R. SHANKS, P. H. SIDLES, AND G. C. DANIELSON, *J. Chem. Phys.* **35**, 298 (1961).
6. W. R. GARDNER AND C. G. DANIELSON, *Phys. Rev.* **93**, 46 (1954).
7. H. R. SHANKS, P. H. SIDLES, AND G. C. DANIELSON, *Adv. Chem. Ser.* **39**, 237 (1963).
8. B. L. CROWDER AND M. J. SIENKO, *J. Chem. Phys.* **38**, 1576 (1963).
9. A. R. MACKINTOSH, *J. Chem. Phys.* **38**, 1991 (1963).
10. W. H. JONES, JR., E. A. GARBATY, AND R. G. BARNES, *J. Chem. Phys.* **36**, 494 (1962).
11. A. FERETTI, D. B. ROGERS, AND J. B. GOODENOUGH, *J. Phys. Chem. Solids* **26**, 2007 (1965).
12. J. M. KELLER, *J. Chem. Phys.* **33**, 232 (1960).
13. A. NARATH AND D. C. WALLACE, *Phys. Rev.* **127**, 724 (1962).
14. R. W. VEST, M. GRIFFEL, AND J. F. SMITH, *J. Chem. Phys.* **28**, 293 (1958).
15. F. J. MORIN, *Bell System Tech., J.* **37**, 1047 (1958).
16. M. J. SIENKO, *J. Am. Chem. Soc.* **81**, 5556 (1959).
17. J. B. GOODENOUGH, *Bull. Soc. Chim. France* **4**, 1200 (1965).
18. B. C. GERSTEIN, L. D. THOMAS, AND D. M. SILVER, *J. Chem. Phys.* **46**, 4288 (1967).
19. R. LATTER, *Phys. Rev.* **99**, 510 (1955).
20. Orion Research, Inc., Cambridge, Massachusetts: M. FRANT AND J. W. ROSS, *Science* **19**, 1553 (1966).
21. B. A. RABY AND W. E. SUNDERLAND, *Anal. Chem.* **39**, 1304 (1967).
22. A. ABRAGAM, "The Principles of Nuclear Magnetism," p. 66, Oxford University Press, London, 1961.
23. W. G. CLARK, Ph.D. Thesis, Cornell University, 1961.
24. W. C. WAYNE, Ph.D. Thesis, Cornell University, 1966.
25. E. R. ANDREWS, "Nuclear Magnetic Resonance," p. 194. Cambridge University Press, London, 1955.
26. A. T. FROMHOLD AND A. NARATH, *Phys. Rev.* **136**, A487 (1964).
27. Y. YAFET AND V. JACCARINO, *Phys. Rev.* **133**, A1630 (1964).
28. Y. OBATA, *J. Phys. Soc. Japan* **18**, 1020 (1963).
29. E. R. ANDREW, *op. cit.*, p. 174 and p. 176.
30. A. ABRAGAM, *op. cit.*, p. 389.
31. J. P. REMEIKA, T. H. GEBALLE, B. T. MATTHIAS, A. S. COOPER, G. W. HULL, AND E. M. KELLY, *Phys. Letters* **24A**, 565 (1967).
32. L. C. HEBEL AND C. P. SLICHTER, *Phys. Rev.* **113**, 1504 (1959).
33. W. LOW, *J. Appl. Phys.* **39**, 1246 (1968).
34. A. J. FREEMAN AND R. E. WATSON, *in* "Magnetism," (H. Suhl and G. Rado, eds.), p. 291. Academic Press, New York, 1965.
35. C. P. SLICHTER, "Principles of Magnetic Resonance," p. 66. Harper, New York, 1963.